

Magnetism in $\text{Co}_{1-x}\text{Fe}_x\text{Sb}_3$ skutterudites from density functional theory

Mikael Råsander^{1,2,*} and Lars Bergqvist^{1,3}

¹*Department of Materials and Nanophysics, KTH Royal Institute of Technology, Electrum 229, SE-164 40 Kista, Sweden*

²*Department of Materials, Imperial College London,
Exhibition Road, London SW7 2AZ, United Kingdom*

³*SeRC (Swedish e-Science Research Centre), KTH, SE-100 44 Stockholm, Sweden*

(Dated: December 17, 2015)

We have investigated the electronic and magnetic properties of $\text{Co}_{1-x}\text{Fe}_x\text{Sb}_3$ skutterudites from density functional theory and Monte Carlo simulations. We find that above a certain threshold in the Fe concentration, somewhere between $x=0.125$ and $x=0.25$, $\text{Co}_{1-x}\text{Fe}_x\text{Sb}_3$ is ferromagnetic with an atomic moment which increases asymptotically towards about $1 \mu_B/\text{Fe}$ and a non-zero Curie temperature which reaches 70 K for FeSb_3 . Ferromagnetism is favored due to a Stoner instability in the electronic structure, where a large density of states at the Fermi-level makes it favorable to form the ferromagnetic ground state.

I. INTRODUCTION

Many materials have been proposed for high efficiency energy conversion in thermoelectric devices, e.g. the clathrates and zintl phases.¹ The skutterudites, generally represented in the form $\text{R}_y\text{M}_4\text{X}_{12}$, where M is a transition metal, e.g. Co or Ir, X is a pnictogen, e.g. As or Sb, and R, if present, is typically a rare-earth element, e.g. La, have shown promise for high thermoelectric conversion efficiency. However, the efficiency for energy conversion, described by the figure-of-merit $ZT = S^2\sigma T/\kappa$, where S is the Seebeck coefficient, σ is the electric conductivity, κ is the thermal conductivity, and T is temperature, is not optimal. The main drawback in the skutterudites, exemplified for instance by CoSb_3 , is that the thermal conductivity is found to be too high.² In order to improve the figure-of-merit of skutterudites, it is possible to include heavy filler elements in the MX_3 skutterudite framework, as in the case of $\text{LaFe}_4\text{Sb}_{12}$, or to alloy the skutterudite phase, as in the case of $\text{Co}_{1-x}\text{Fe}_x\text{Sb}_3$.³⁻⁵

$\text{Co}_{1-x}\text{Fe}_x\text{Sb}_3$ has received attention since doping of CoSb_3 leads to more favourable thermoelectric properties, e.g. a larger carrier concentration and lowered thermal conductivity.³⁻⁵ We note that studies on $\text{Co}_{1-x}\text{Fe}_x\text{Sb}_3$ contain rather small amounts of Fe; the maximum Fe content has been varied in these studies from $x = 0.1^3$ to 0.4^4 mostly since larger amounts of Fe is not possible to incorporate into the skutterudite phase with traditional means, due to the metastability of FeSb_3 which separates into FeSb_2 and Sb.⁶ Recently, however, attention has been given to pure FeSb_3 since it has been shown that it is possible to synthesize thin FeSb_3 films using the modulated elemental reactant method (MERM).⁶⁻⁸

Following the synthesis of FeSb_3 films, density functional calculations have revealed that the pure FeSb_3 system is a ferromagnet with a low transition temperature;⁹ much lower than room temperature and also much lower than the thermoelectric operating temperatures suggested for these compounds. FeSb_3 was also found to be softer than CoSb_3 , for both the elastic constants and

the lattice dynamics, which suggests that the thermal conductivity in this material is lower than in CoSb_3 .^{7,9} It was also shown by Råsander *et al.* that magnetism is essential in order to have a dynamically stable system.⁹ Interestingly, Fe has been found to be paramagnetic in $\text{Co}_{1-x}\text{Fe}_x\text{Sb}_3$,³ as well as in other antimonide skutterudites.^{3,10-12} However, there are ferromagnetic skutterudites found in the literature, e.g. $\text{NaFe}_4\text{Sb}_{12}$ and $\text{KFe}_4\text{Sb}_{12}$,^{13,14} and ferromagnetic behavior should therefore not be surprising.

Experimentally, FeSb_3 was found to be paramagnetic with an effective paramagnetic moment of $0.57(6) \mu_B/\text{f.u.}$ ⁷ However, density functional theory calculations do obtain a ferromagnetic solution for the ground of FeSb_3 .^{8,9,15} In fact, FeSb_3 is found to be a near half-metal in its ferromagnetic ground state⁹ while experiments performed by Möchel *et al.*⁷ obtain a small gap of $16.3(4) \text{ meV}$. This behavior agrees with a recent hybrid density functional study of Lemal *et al.*¹⁶ which finds a small gap of 33 meV . In their study Lemal *et al.* also determine the FeSb_3 phase to be antiferromagnetic with an estimated Néel temperature of 6 K and an atomic magnetic moment of $1.6 \mu_B/\text{Fe}$. The latter should be compared with previously reported ferromagnetic and antiferromagnetic moments of $1.0 \mu_B/\text{Fe}$ and $1.1 \mu_B/\text{Fe}$, respectively.⁹ Note, however, that the experiment performed by Daniel *et al.*⁸ find the FeSb_3 films to have a metallic conductivity and therefore no gap, so the experimental situation regarding FeSb_3 is not completely clear. What is clear, however, is that magnetism plays an important role in FeSb_3 and, therefore, it should also be of importance in $\text{Co}_{1-x}\text{Fe}_x\text{Sb}_3$. In order to reconcile the discrepancy between experimental and theoretical results regarding the magnetic properties, it was suggested by Xing *et al.*¹⁵ that a possible overestimation of the magnetic properties compared to experiments could possibly be due to spin fluctuations associated with a nearby quantum critical point that are strong enough to renormalize the mean-field magnetic state predicted by density functional calculations,¹⁵ similar to what is observed in ferropnictides.¹⁷ Such behavior has indeed been observed in $\text{NaFe}_4\text{Sb}_{12}$ and $\text{KFe}_4\text{Sb}_{12}$ where exper-

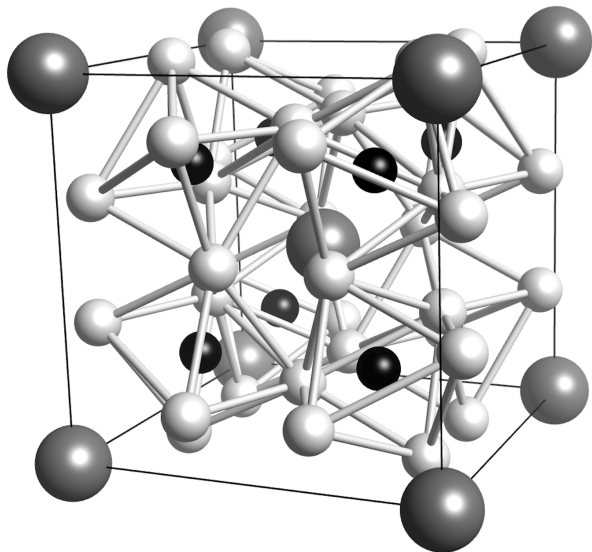


FIG. 1. Illustration of the crystal structure of the skutterudite structure. Fe (black spheres) is residing inside canted octahedral cages of Sb (white spheres). Filler atoms are presented by large grey spheres.

imentally ordered moments of $\sim 1 \mu_B$ is found compared to $\sim 3 \mu_B$ predicted by theory.^{13,14}

In this paper, we provide results from density functional calculations on $\text{Co}_{1-x}\text{Fe}_x\text{Sb}_3$ in order to provide a further understanding of the magnetic properties of these systems. Specifically, we have calculated the transition temperatures based on a first principles approach. We show that, among other things, the magnetic moments are to a great extent localised on the Fe atoms and the transition temperatures are low throughout the whole composition range in $\text{Co}_{1-x}\text{Fe}_x\text{Sb}_3$.

The paper is outlined as follows: In section II we present the details of the calculations, in section III we present the results of our study and finally in section IV we summarise our finding and draw conclusions.

II. COMPUTATIONAL DETAILS

The binary skutterudite structure has a unit cell containing four formula units with body centered cubic lattice vectors and belongs to the space group $\text{Im}\bar{3}$ (No. 204), where metal atoms and pnictogen atoms occupy the 8c and 24g positions respectively. The pnictogen atoms occupy the general position $(0,y,z)$. The skutterudite framework, i.e. MX_3 , contains large voids at the 2a positions of the lattice. In Fig. 1 we show the conventional unit cell of the skutterudite structure (8 formula units) with the voids, at $(0,0,0)$ and $(\frac{1}{2}, \frac{1}{2}, \frac{1}{2})$, filled with a rare-earth element.

In order to calculate the magnetic properties of $\text{Co}_{1-x}\text{Fe}_x\text{Sb}_3$, we have made use of a combination of first principles density functional calculations. Structural

TABLE I. Comparison of the evaluated lattice constants and crystallographic y and z values for the Sb atoms in FeSb_3 and CoSb_3 for spin-polarized (in ferromagnetic (FM) and anti-ferromagnetic (AFM) configurations) and non spin-polarized (NSP) calculations. The Vegard's law value is extracted from the study on $\text{Co}_{1-x}\text{Fe}_x\text{Sb}_3$ by Yang *et al.*³

| System | | a (Å) | y | z |
|-----------------|-----------------------------------|---------|-------|-------|
| FeSb_3 | NSP | 9.153 | 0.327 | 0.160 |
| FeSb_3 | FM | 9.178 | 0.331 | 0.160 |
| FeSb_3 | AFM | 9.166 | 0.331 | 0.159 |
| FeSb_3 | Expt. ⁶ | 9.176 | 0.340 | 0.162 |
| FeSb_3 | Expt. ($T = 10$ K) ⁷ | 9.212 | 0.340 | 0.158 |
| FeSb_3 | Expt. ($T = 300$ K) ⁷ | 9.238 | 0.340 | 0.157 |
| FeSb_3 | Vegard's law ³ | 9.126 | - | - |
| CoSb_3 | NSP | 9.115 | 0.333 | 0.160 |
| CoSb_3 | Expt. ²¹ | 9.039 | 0.335 | 0.158 |

properties of CoSb_3 and FeSb_3 have been determined using the Projector augmented wave (PAW) method¹⁸ as it is implemented in the Vienna ab initio simulation package (VASP).^{19,20} The Perdew-Burke-Ernzerhof (PBE) generalised gradient approximation was used for the exchange-correlation energy functional. Further details regarding these calculations can be found in Ref. 9. The resulting structural parameters are shown in Table I. As can be seen in Table I FeSb_3 has a larger lattice constant than CoSb_3 . However, the y and z parameters for the Sb atoms are very similar in FeSb_3 and CoSb_3 . We have therefore chosen to apply a Vegard's law behaviour for the intermediate phases in $\text{Co}_{1-x}\text{Fe}_x\text{Sb}_3$, for $0 < x < 1$, with the y and z parameters fixed. A Vegard's law type of behaviour is also supported by Yang *et al.*³ in their study of $\text{Co}_{1-x}\text{Fe}_x\text{Sb}_3$, for $0 \leq x \leq 0.1$, where such a behaviour was observed. The lattice constant for FeSb_3 labelled Vegard's law in Table I is extrapolated from the result of Yang *et al.*³

In addition to the previously mentioned PAW calculations, the electronic and magnetic properties of $\text{Co}_{1-x}\text{Fe}_x\text{Sb}_3$ has been investigated using the Korringa-Kohn-Rostoker (KKR) method using the SPR-KKR software package²². The electronic states were treated fully relativistic by solving the Dirac equation employing a basis set consisting of s , p and d orbitals. The local spin density approximation (LSDA) was used for the exchange correlation functional and the shape of the potential was treated using the atomic sphere approximation (ASA) with additional empty spheres to minimize the overlap of the different muffin-tin spheres centered on the atomic sites. The coherent potential approximation (CPA)²³, was employed to treat disorder effects, i.e mixing of Co and Fe. Magnetic moments and exchange parameters within a Heisenberg model were obtained from the magnetic force theorem using the Lichtenstein-Katsnelson-Antropov-Gubanov (LKAG) formula^{24,25} and then used as input for subsequent Monte Carlo simulations using the UppASD package²⁶. Our accuracy in determining

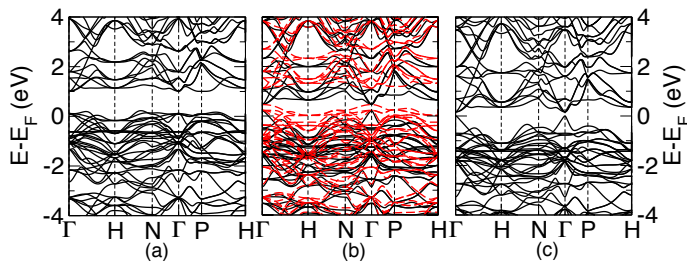


FIG. 2. (Color online) Calculated band structures of (a) NSP FeSb₃, (b) FM FeSb₃ (c) and CoSb₃. The Fermi-level, E_F , is found at 0 eV. In (b) the spin-up band are plotted with solid (black) lines and the spin-down bands are plotted with dashed (red) lines. For more details, see Ref. 9.

the transition temperatures is estimated to give an error of about ± 3 K.

III. RESULTS

We begin with a discussion of the electronic structure of the two endpoint systems in our study, namely CoSb₃ and FeSb₃. The electronic structure of these compounds have been discussed in detail before^{8,9,15} and we will here briefly recapture the results of previous studies. The band structures in CoSb₃ and FeSb₃ are shown in Fig. 2. CoSb₃ is a semiconductor with a small direct gap of 0.17 eV. FeSb₃ on the other hand is a near half-metal ferromagnet (FM) where the spin-up channel is almost full. Non-spin polarised (NSP) FeSb₃ has a large number of bands with rather small dispersion close to the Fermi-level which according to the Stoner criterion makes it favourable for the system to have a ferromagnetic ground state.⁹ The magnetic moment in FM FeSb₃ is $\sim 1.0 \mu_B/\text{Fe}$ ^{9,15} largely localised to the Fe atoms.

In Fig. 3 we show the calculated Bloch spectral function (BSF) $A(E, \mathbf{k})$ for Co_{0.75}Fe_{0.25}Sb₃ within CPA. The

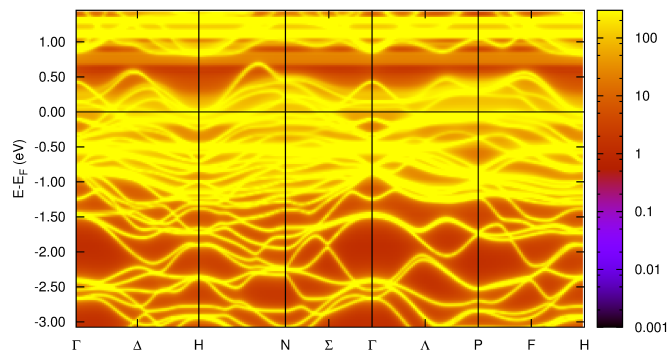


FIG. 3. Calculated Bloch spectral function (BSF) for Co_{0.75}Fe_{0.25}Sb₃ (spin polarized calculation) along directions of high symmetry in the Brillouin zone. The y-axis represents the energy in eV and the Fermi-level, E_F is found at 0 eV.

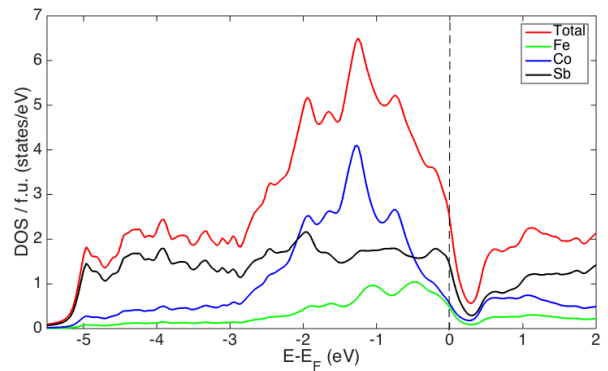


FIG. 4. Calculated NSP density of states (DOS) / formula unit (f.u) for Co_{0.75}Fe_{0.25}Sb₃. The Fermi level, E_F , is marked with a vertical dashed line.

BSF is a suitable way of analyzing band structures in disordered systems and can be seen as a wave vector \mathbf{k} -resolved density of states (DOS) function. For ordered systems the $A(E, \mathbf{k})$ is a δ -like function at energy E and can be used as an alternative way to calculate band structures, as in Fig. 2. However, for disordered systems, in addition to the energy, the BSF also has a broadening associated to the amount of disorder in the system. From Fig. 3, it is clear that disorder mostly takes place close to Fermi level since the electron bands are most diffuse there and several bands are crossing the Fermi level. The underlying mechanism for this are explained in the following way. Adding Fe to CoSb₃, d -bands from Co and Fe start to cross the Fermi level and the density of states increases making it favourable to form a ferromagnetic ground state and this effect becomes stronger as the Fe content increases.

This is analyzed further by calculating the NSP density of states of Co_{0.75}Fe_{0.25}Sb₃, shown in Fig. 4. According to the Stoner criteria of ferromagnetism, a material may lower its total energy by exchange splitting of the bands, i.e. become ferromagnetic, if $I \cdot D(E_F) > 1$, where $D(E_F)$ is the NSP density of states at the Fermi level, E_F , and I is the Stoner exchange integral. I has been calculated for most elements in the periodic table and its value is typically around 0.7-0.8 eV²⁷ without much variation. If the Stoner criteria is assumed to hold, it means that $D(E_F)$ must exceed ≈ 1.3 states/eV in order to promote ferromagnetism. From Fig. 4, taking only into account Fe and Co states, $D(E_F)$ is around 1.1 states/eV which is on the borderline to become ferromagnetic. If also Sb states are taken into account, or partially through hybridization with Fe and Co states, then the Stoner criteria is fulfilled and ferromagnetism is expected. The analysis is somewhat simplified but it indicates that doping with Fe of CoSb₃ promotes a magnetic state, which is indeed also found in the full electronic structure calculations.

In Fig. 5 and Table II we show the calculated magnetic moments and transition temperatures for $0 \leq x \leq 1$. We note that the formation of a magnetic moment sets in for

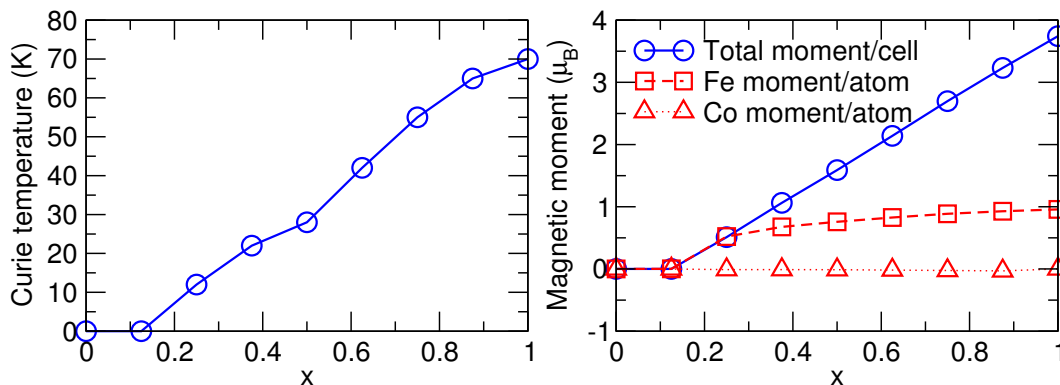


FIG. 5. Calculated transition temperatures (left) and magnetic moments (right) for $\text{Co}_{1-x}\text{Fe}_x\text{Sb}_3$. Note that a summation of the Fe moment in the case of $x = 1$ will give a moment that is larger than the total moment shown in the figure.

$x > 0.125$. After this point we find a linear increase in the total magnetic moment with increasing Fe concentration. The moments localised on the Fe atoms increase drastically for $0.125 \leq x \leq 0.25$ and thereafter the increase is much less dramatic as the Fe content increases. The Fe moment has its maximum value of $0.96 \mu_B$ for $x = 1$, i.e. for FeSb_3 . We note that the Fe moments make up most of the total moments. The moments localised on the other atoms work towards lowering the total moment in the system. This is represented by the very small negative Co moments shown in Fig. 5 and Table II.

In order to investigate the build up of magnetism for small Fe concentrations further, we have performed calculations on a single Fe atom substituting Co in a $3 \times 3 \times 3$ CoSb_3 unit cell using the PAW method. The effective concentration of Fe in CoSb_3 is in this case less than 1%. We find that for this low concentration the total magnetic moment is zero and the moments on the different atoms are also zero which is in agreement with our ASA calculations. This suggests that a rather substantial concentration of Fe is necessary for the formation of a magnetic moment in the system.

The linear increase in the total magnetic moment with increasing Fe content is reflected in the magnetic transition temperatures shown in Fig. 5 and Table II. For $x \leq 0.125$ the transition temperature is zero and thereafter we find a monotonous increase of the transition temperature as the amount of Fe increases. The transition temperature reaches its maximum for $x = 1$, i.e. for pure FeSb_3 for which $T_c = 70$ K. We note that the T_c of FeSb_3 has been reported to be 175 K.⁹ However, the higher transition temperature in Ref. 9 was obtained from a scalar relativistic full-potential calculation. Here we used full relativistic calculations within the ASA. It is often found that using the scalar relativistic full-potential approach yield stronger magnetic interactions and consequently higher transition temperatures compared to the full relativistic ASA approach utilised here, due to the additional spin-flip terms that mix the majority and minority spin channels in the latter case. Even so, we find that overall the magnetic interactions yield rather

TABLE II. Calculated magnetic moments for the skutterudite cell (m_{tot}), magnetic moments projected on to Co (m_{Co}) and Fe (m_{Fe}) atoms from full relativistic ASA calculations, as well as calculated transition temperatures obtained by Monte Carlo simulations (T_c). The errors in the transition temperatures are about ± 3 K.

| x | $m_{Co} (\mu_B)$ | $m_{Fe} (\mu_B)$ | $m_{tot} (\mu_B)$ | T_c (K) |
|-------|------------------|------------------|-------------------|-----------|
| 0.000 | 0.00 | - | 0.00 | 0 |
| 0.125 | -0.00 | 0.00 | 0.00 | 0 |
| 0.250 | -0.01 | 0.52 | 0.51 | 12 |
| 0.375 | -0.01 | 0.68 | 1.06 | 22 |
| 0.500 | -0.01 | 0.76 | 1.59 | 28 |
| 0.625 | -0.02 | 0.83 | 2.14 | 42 |
| 0.750 | -0.02 | 0.89 | 2.70 | 55 |
| 0.875 | -0.03 | 0.93 | 3.23 | 65 |
| 1.000 | - | 0.96 | 3.74 | 70 |

low transition temperatures; much lower than possible operating temperatures of $\text{Co}_{1-x}\text{Fe}_x\text{Sb}_3$ -based thermoelectric devices. As an additional test, we also performed self-consistent total energy calculations of FeSb_3 in the paramagnetic state using the disordered local moment (DLM) magnetic state within CPA. The total energy of the DLM state was found to be ≈ 15 meV/f.u higher than the FM state. The transition temperature in the mean field approximation (MFA) has the expression $k_B T_c^{MFA} = \frac{2}{3} \Delta E$, and using the energy difference between FM and DLM state yields 113 K, consistent with the Monte Carlo values using the exchange parameters since MFA always overestimate the value of the transition temperature.

IV. SUMMARY AND CONCLUSIONS

We have performed first principles density functional calculations in order to investigate the electronic and magnetic properties of $\text{Co}_{1-x}\text{Fe}_x\text{Sb}_3$ for $0 \leq x \leq 1$. We find that for low Fe concentrations ($x \leq 0.125$) magnetism is non-existent or at least very weak. For larger

Fe concentrations we find that both the magnetic moment and transition temperatures in $\text{Co}_{1-x}\text{Fe}_x\text{Sb}_3$ increase monotonically with increasing Fe content. The maximum transition temperature of 70 K is found for FeSb_3 . The ferromagnetism in $\text{Co}_{1-x}\text{Fe}_x\text{Sb}_3$ is driven by the build up of states close to the Fermi-level with increasing Fe content which makes it more and more favourable to form a ferromagnetic solution. We note that the observed paramagnetic behavior observed in $\text{Co}_{1-x}\text{Fe}_x\text{Sb}_3$ ³ is found for Fe concentrations where we find no, or possibly very weak, ferromagnetism. If ferromagnetism is weak it is likely that a transition to a paramagnetic state occurs at low temperature. In the

case of FeSb_3 , we believe that the observed paramagnetic behavior can be explained by spin fluctuations that renormalize the magnetic state obtained within density functional theory, as suggested by Xing *et al.*¹⁵

V. ACKNOWLEDGEMENTS

This work was financed through the VR (the Swedish Research Council) and GGS (Göran Gustafsson Foundation). The computations were performed on resources provided by the Swedish National Infrastructure for Computing (SNIC) at the National Supercomputer Centre in Linköping (NSC).

-
- * m.rasander@imperial.ac.uk
- ¹ G. J. Snyder and E. S. Toberer, Nat. Mater. **7**, 105 (2008).
 - ² L. Hammerschmidt, S. Schlecht, and B. Paulus, Phys. Stat. Solidi A **210**, 131 (2013).
 - ³ J. Yang, G. P. Meisner, D. T. Morelli, and C. Uher, Phys. Rev. B **63**, 014410 (2000).
 - ⁴ S. Katsuyama, Y. Shichijo, M. Ito, K. Majima, and H. Nagai, J. Appl. Phys. **84**, 6708 (1998).
 - ⁵ P. Amornpitoksuk, D. Ravot, A. Mauger, and J. C. Tedenac, J. Alloy Compd **440**, 295 (2007).
 - ⁶ M. D. Hornbostel, E. J. Hyer, J. Thiel, and D. C. Johnson, J. Am. Chem. Soc. **119**, 2665 (1997).
 - ⁷ A. Möchel, I. Sergueev, N. Nguyen, G. J. Long, F. Grandjean, D. C. Johnson, and R. P. Hermann, Phys. Rev. B **84**, 064302 (2011).
 - ⁸ M. V. Daniel, L. Hammerschmidt, C. Schmidt, F. Timmermann, J. Franke, N. Jöhrmann, M. Hietschold, D. C. Johnson, B. Paulus, and M. Albrecht, Phys. Rev. B **91**, 085410 (2015).
 - ⁹ M. Räsander, L. Bergqvist, and A. Delin, Phys. Rev. B **91**, 014303 (2015).
 - ¹⁰ M. E. Danebrock, C. B. H. Evers, and W. Jeitschko, J. Phys. Chem. Solids **57**, 381 (1996).
 - ¹¹ B. C. Sales, D. Mandrus, B. C. Chakoumakos, V. Keppens, and J. R. Thompson, Phys. Rev. B **56**, 15081 (1997).
 - ¹² D. A. Gajewski, N. R. Dilley, E. D. Bauer, E. J. Freeman, R. Chau, M. B. Maple, D. Mandrus, B. C. Sales, and A. H. Lacerda, J. Phys.: Condens. Matter **10**, 6973 (1998).
 - ¹³ A. Leithe-Jasper, W. Schnelle, H. Rosner, N. Senthil Kumar, A. Rabis, M. Baenitz, A. Gippius, E. M. J. A. Mydosh, and Y. Grin, Phys. Rev. Lett. **91**, 037208 (2003).
 - ¹⁴ A. Leithe-Jasper, W. Schnelle, H. Rosner, M. Baenitz, A. Rabis, A. A. Gippius, E. N. Morozova, H. Borrmann, U. Burkhardt, R. Ramlau, U. Schwarz, J. A. Mydosh, Y. Grin, V. Ksenofontov, and S. Reiman, Phys. Rev. B **70**, 214418 (2004).
 - ¹⁵ G. Xing, X. Fan, W. Zheng, Y. Ma, H. Shi, and D. J. Singh, Sci. Rep. **5**, 10782 (2015).
 - ¹⁶ S. Lemal, N. Nguyen, J. de Boer, P. Ghosez, J. Varignon, B. Klobes, R. P. Hermann, and M. J. Verstraete, Phys. Rev. B **92**, 205204 (2015).
 - ¹⁷ I. I. Mazin, M. D. Johannes, L. Boeri, K. Koepernik, and D. J. Singh, Phys. Rev. B **78**, 085104 (2004).
 - ¹⁸ P. E. Blöchl, Phys. Rev. B **50**, 17953 (1994).
 - ¹⁹ G. Kresse and J. Furthmüller, Phys. Rev. B **54**, 11169 (1996).
 - ²⁰ G. Kresse and D. Joubert, Phys. Rev. B **59**, 1758 (1999).
 - ²¹ T. Schmidt, G. Kliche, and H. D. Lutz, Acta Cryst. C **43**, 1678 (1987).
 - ²² H. Ebert, D. Ködderitzsch, and J. Minar, Rep. Prog. Phys. **74**, 096501 (2010).
 - ²³ P. Soven, Phys. Rev. **156**, 809 (2011).
 - ²⁴ A. I. Lichtenstein, M. I. Katsnelson, and V. A. Gubanov, J. Phys. F: Met. Phys. **14**, L125 (1984).
 - ²⁵ A. I. Lichtenstein, M. I. Katsnelson, V. P. Antropov, and V. A. Gubanov, J. Magn. Magn. Mater. **67**, 65 (1987).
 - ²⁶ B. Skubic, J. Hellsvik, L. Nordström, and O. Eriksson, J. Phys. Condens. Matter **20**, 315203 (2008).
 - ²⁷ J. F. Janak, Phys. Rev. B **16**, 255 (1977).